Microfibrous extracellular matrix enhances in vitro modeling of the liver hepatocytes by modulating metabolism and integrin expression

Tianjiao Huang[1], Curtis G. Jones[2], Jay H. Chung[1] and Chengpeng Chen[2]*

1. Laboratory of Obesity and Aging Research, Cardiovascular Branch, National Heart Lung and Blood Institute, National Institutes of Health, Bethesda, Maryland 20892, USA

2. The Department of Chemistry and Biochemistry, University of Maryland Baltimore County, MD, USA, 21250

*corresponding to:

Dr. Chengpeng Chen

cpchen@umbc.edu

+1-4104553053

Introduction

The liver carries out a number of essential functions, including blood detoxification, protein synthesis, regulation of energy balance, and production of other biochemicals to maintain the whole-body homeostasis[1]. In addition to these physiological functions, the liver is also the main site of drug metabolism, making it vulnerable to drug toxicity; indeed, hepatotoxicity is one of the leading causes for drug failure[2]. Thus, detecting the potential for hepatotoxicity of a drug at the early stage of drug development/screening will minimize the failure rate and, therefore, the cost of bringing a drug into the market. Therefore, hepatic models are invaluable tools in drug discovery and development.

There are two general families of hepatic models used in research: *in vivo* and *in vitro*. The obvious advantage of the *in vivo* animal models such as rodents is the conservation of the organ and system level complexity to observe the overall responses of a liver[3]. However, animal models pose other challenges. First, the throughput of animal models is usually low because of the high time, labor, and monetary costs[4]. Also, animal models typically test a single drug each time to avoid interferences, which further limits the throughput[5]. In addition, very high doses of compounds, sometimes orders of magnitude higher than those humans are exposed to[6] are required for animal experiments to generate more evident results.

In vitro models are tissue/cell culture-based methodologies, which can circumvent the throughput, cost, and dosing issues of *in vivo* models[6]. For example, hepatocytes can be batch cultured in a multi-well plate treated with various drugs of different doses in one experiment. Three types of biocomponents are mainly used to fabricate an *in vitro* hepatic model: liver slices, primary hepatocytes, and hepatic cell lines. Despite the physiological relevance of liver tissue slices that retain liver structures and the cell types, the functions of the hepatocytes start decaying after 6 hours of tissue isolation[7]. Primary hepatocytes have similar enzyme activities as hepatocytes in whole liver, but the hepatocyte function declines fast during culture, and these cells are not available to every laboratory[8]. Immortalized hepatic cell lines such as Huh7 and HepG2 are long-lasting, retain liver-specific functions, and are easy to maintain[9]. Therefore, these cell lines have been widely-used, especially for high throughput initial drug screenings[10]. However, a significant number of findings from cell line-based models were not reproducible in subsequent preclinical and clinical studies[10], reflecting the inadequacy of the cell line model[11].

In order for the hepatic cell lines to better simulate liver function, the cellular environment is critical. However, cell lines are typically cultured as a 2D monolayer in a container (e.g., flasks),

which cannot mimic the 3D microenvironment of the cells in tissue[12]. In tissues, cells rest on and interact with the 3D extracellular matrix (ECM), which contain fibrous microstructures and can regulate cell behaviors and functions[13]. Therefore, incorporating ECMs into tissue culture models may provide a more physiological environment. With the advancement of material science and microfabrication technologies, various *in vitro* 3D hepatic models have been reported[14-16]. Hepatocytes naturally aggregate to form spheroids in proper microcontainers[17]; thus, microwell platforms are utilized for 3D hepatic spheroids culture. For example, Bhise et al. fabricated a microwell array using stamps on polydimethylsiloxane (PDMS) with successful spheroids formation of ~200 μm diameter, which showed consistent production of albumin and appropriate responses to drugs[18]. Hydrogels–networks of polymer chains that are highly hydrated are also prevailing as a 3D matrix for cell culture[19, 20]. Precursors of hydrogels premixed with cells can be cured under physical (e.g., UV radiation) and chemical (e.g., crosslinker) conditions with desired shapes and dimensions via micromolds or bio-3D-printing[21-23]. Electrospinning is another technology to fabricate 3D fibrous ECM, which applies a high voltage (kV range) to turn a polymer solution to micro-/nano-fibers with tunable fiber and pore sizes[24]. A myriad of cell types including hepatocytes[25] have been successfully 3D cultured on electrospun fibers showing improved functions[26-29].

These approaches offer a great promise for the development of functional 3D liver models. However, most of them have only focused on the few fingerprint functions of hepatocytes, including protein synthesis and secretion (mainly albumin)[18], CYP activities[30], and responses to certain drugs/toxins[11]. While these results are meaningful and informative, none of them explores the impacts of an ECM on the basic metabolic parameters of hepatocytes such as energy and amino acid production. Here, we present our findings on energy metabolites and amino acid levels in hepatocytes culture in 3D vs. 2D. We found that the levels of metabolites important for energy metabolism (glycolysis + Krebs cycle) in Huh7s are significantly lower in those grown on the fibrous ECM compared to those on a 2D flat surface, suggesting that the ECM decreases energy metabolism. The mechanism by which the ECM regulates Huh7 basic metabolisms was also investigated. Fibrous ECM downregulates integrins, the membrane ECM receptor that transduces ECM biophysical cues to intracellular signaling[31], which in turn reduces energy metabolism by increasing cAMP (cyclic adenosine monophosphate) production and the activity of its effector PKA (protein kinase A)[32-34]. Cell morphology analyses also support the role of the integrins in the ECM effect.

Experimental

Fabrication of silk fibroin fibers. Silk fibroin was extracted from silkworm cocoon following the well-established method by Rockwood[35]. Purified and lyophilized silk fibroin was dissolved in HFP (hexafluoroisopropanol; Millipore-Sigma, MO) at a concentration of 6% (w/v). The solution was loaded in a 3 mL syringe coupled with a 20-gauge blunt needle. A syringe pump was used to deliver the fibroin solution at 1mL/hr. A voltage of 25 kV was applied to the syringe needle to generate electrospun fibers, which was deposited on a grounded stainless-steel plate. after 2 hours of electrospinning, a layer of silk fibroin fibers of ~100 μm thick was collected.

Preparation of the cell-culture plate. The electrospun fibers was peeled off from the steel plate and spread on a polystyrene sheet (250 μm thick). Deionized water was sprayed on the fibers to further spread the fiber layer on the polystyrene. After over-night drying, the two layers are bounded likely due to intermolecular forces. The reason to use the polystyrene sheet is because the thin and flexible electrospun fiber layer can be compromised easily (e.g., by pipetting liquid onto it) and supporting it on a sturdy stratum (the polystyrene) can circumvent the issue. A laser cutter was then applied to cut discs of 34.5 mm out of the fiber-polystyrene sheet, which can fit in a 6-well plate. The cutting edge also fuses the fiber layer onto polystyrene. Three discs with the fibers were placed in three wells of a 6-well plate, while the remaining three well contain discs of flat polystyrene as controls for 2D monolayer culture. All discs were sterilized by being soaked in 70% ethanol for 30 min, followed by air drying in UV. Conducting control experiments on the same plate under identical cell seeding, culture, and sampling conditions will reduce variance.

Huh7 cell culture and sampling. Huh7 cells (ATCC, VA) with passage numbers between 2 and 5 were used. DMEM media supplemented with 10% FBS and 1% pen-strep was applied for culture. A flask (T-75) of cells was trypsinized, centrifuged, and resuspended at a density of 0.5 million cells/mL. Next, 2 mL of the cell suspension was added to each well containing either fibrous or flat ECM. This step was to seed the cells on the discs; after 2 hours, 4 mL of fresh media was added to each well. Media was changed every 24 hours until confluency (3 days).

To take cell lysates for intracellular metabolites quantitation, the media was aspirated in each well, followed by washing 3 times using PBS buffer (Millipore-Sigma, MO). After that, 400 μL of LCMS grade water at 0 °C (Millipore-Sigma, MO) was added to each well. An ultrasonic homogenizer probe was used to lyse the cells in each well for 1 min. An aliquot of 200 μL of the lysate was taken for BCA protein assay, as a measurement of cell numbers in each well for

subsequent data normalization. The remaining lysates was mixed with 800 µL acetonitrile/methanol (50/50; v/v) containing 10 µM ^{13}C-threonine (as internal standard for LC-MS analyses, purchased from Cambridge Isotope Laboratories, Inc. Tewksbury, MA) and vortex mixed for 30s. Then samples were incubated for 1h at -20 °C to precipitate proteins, which were then centrifuged at 14,000 rpm (Eppendorf, Centrifuge 5424R, Hauppauge, NY) at 4 °C. The supernatant was transferred to another clean vial, followed by lyophilizing (Savant from Thermo Scientific, Waltham, MA). The dry extracts were reconstituted in 15 µL in 0.1% Formic acid LCMS grader water and transfer to LCMS analysis.

LC-MS analyses of the intracellular metabolites of interest. LCMS analysis was performed with an Agilent G6530C LC QTOF system equipped with the capillary HPLC 1260 Infinity series. For both positive and negative detection modes, a full scan range of 50 to 1000 m/z with mass accuracy of 2 ppm was performed. For the positive mode, ESI ion source parameters are: gas temperature 320 °C, drying gas 10 L/min, nebulizer 30 psi and capillary voltage 3500 V. The fragmentor, skimmer and OCT1 RF Vpp were set to 110, 65 and 750 volts, respectively. For the negative mode, ESI ion source parameters are: gas temperature 300 °C, drying gas 10 L/min, nebulizer 30 psi, and capillary voltage 2700 V. The fragmentor, skimmer and OCT1 RF Vpp was set to 90, 65 and 750 volts, respectively.

A C18 column (Luna® Omega 1.6 µm, PS 100 Å with inner diameter of 100 × 2.1 mm) was used via the following gradient: mobile phase A was 0.1 % formic acid in water, mobile phase B was LCMS grade methanol (fisher scientific, Hampton, NH). At positive mode, gradient started with 100% A at 0 min, and decreased to 0% A at 15 min. The A phase was remained at 0% till 25 min, followed by being increased to 100% at 30 min and hold until 45 min. Flow rate was set at 30 µL/min. For negative mode, the gradient was same but with a flow rate of 40 µL/min. An aliquot of 5 µL of samples was injected to the column by an autosampler, followed by MS measurement.

Immunoblotting. Cell lysate were harvested by adding 100 µL of RIPA buffer (radioimmunoprecipitation assay buffer with 150 mM sodium chloride, 1.0% NP-40, 0.5% sodium deoxycholate, 0.1% SDS and 50 mM Tris, pH 8.0) with complete protease inhibitor cocktail (Abcam, Cambridge, MA, USA), sonicated on ice on the day of analysis. The protein concentration of the lysates was determined by Coomassie protein assay kit following to the manufacturer's recommendation (Thermo Scientific, USA). Cell lysates with 25 µg of total protein were subjected to 7 % SDS-polyacrylamide gels (Bio-Rad, Hercules, CA, USA). After electrophoresis, proteins were transferred into nitrocellulose membranes (Bio-Rad, Hercules, CA, USA). The membranes were blocked in PBST buffer (PBS with 0.1% Tween-20) containing 2%

non-fat dry milk power for 30 min at room temperature. Subsequently the membranes were incubated over night with rabbit-monoclonal anti- Phospho-CREB (Ser133), rabbit-polyclonal anti-Integrin β1 and rabbit-polyclonal anti-β-Actin (1:1000) at 4°C. After washing in PBST buffer, the membranes were incubated with horseradish peroxidate-conjugated anti-rabbit antibodies (1:1000). Immunoreactivity was detected using an Amersham Imager (GE Healthcare, MA, USA). The band intensity was related to β-Actin.

Data analyses. Peak areas of the analytes of interest was analyzed by MassHunter Qualitative Analysis Version B.10, which will first be normalized to the internal standard (^{13}C-threonine). The data were further normalized by cell numbers in each culture well (by the gross protein assay). Next, the normalized peak area of a metabolite from cells cultured on the fibrous ECM was divided by that from cells on the flat surface, so that percentage of change of each metabolite can be elucidated. A total of 15 replicates were conducted, and significant difference was considered only when p values are smaller than 0.05.

Results and discussion

Human liver cell lines derived from hepatic carcinomas such as HepG2 and Huh7 have been widely applied in toxicity test, drug screening, and physiological studies[36-38]. However, discrepancies exist between the cell lines and hepatocytes in the liver, making many *in vitro* results irreproducible in subsequent animal and clinical trials[39, 40]. Accumulating evidence indicates that the way the cells are cultured *in vitro* can be a cause of the discrepancies[19, 41]. Cells grown in a 2D monolayer in a container (e.g., flasks) or on a surface (e.g., porous membrane) cannot recapitulate the *in vivo* microenvironment[42]. Cell *in vivo* are on 3D microfibrous ECMs, which can modulate cell behaviors and functions via two mechanisms[43]: 1) enhancing cell-cell interactions by defining the physical space between cells; 2) directly affecting cellular pathways via ECM receptors such as integrins. A considerable volume of literature has demonstrated the importance of 3D ECM for *in vitro* hepatocyte cultures/studies[40]–"the third dimension bridges the gap between cell culture and live tissue"[44]. Here, we report our findings that a 3D fibrous ECM can modulate Huh7 cell lines towards physiological relevance by modulating basic metabolism and integrins expression.

The ECM, controls, and research design

Electrospun fibers have been successfully utilized as the ECM in 3D cell culture[23, 27, 45]. Therefore, we used microfibers electrospun from silk fibroin[24, 35] as the hepatic ECM here. We deposited a layer of fibers (50 μm thick) on a polystyrene sheet, which was laser cut to discs that fit in a 6-well plate (**Fig. 1A**). The laser cutting can also fuse the edges of the fibers and the polystyrene to permanently bind the two layers. The polystyrene acts as a support structure so that the flimsy/flexible fibers will not be compromised when adding and/or removing media. **Fig. 1B** is an SEM (scanning electron microscope) view of the microfibers, the average diameter of which is 0.78±0.37μm (mean ± stdev), with most fibers distributed in the 0.50-1.00 μm range (inset histogram). Although microtiter plates with embedded fibrous bottoms are available, our modular protocol has unique advantages: 1) as **Fig.1C** shows, both experimental (3D fibrous) and control (2D flat) ECMs can be included in the same plate, so that cells from the same parental flask can be seeded, cultured, and studied in the same environment, reducing possible culture variances; 2) the fibrous discs can be batch prepared from one electrospinning for a whole study to ensure exactly identical ECM conditions; and 3) with an all-in-one plate, the whole plate has to be discarded even only a few wells were used while our modular design is more cost-efficient because the well numbers and the properties of the ECMs are customizable.

The ECM modulates energy metabolism in Huh7 cells toward physiological relevance

A major difference between the Huh7 cell line and hepatocytes *in vivo* is energy metabolism[46]. As a carcinoma cell line, Huh7 has high glycolysis and highly active Krebs cycle[47], which is the central route for intracellular oxidative phosphorylation, and is important for cellular bioenergetic, biosynthetic, and redox homeostasis[48]. Moreover, elevated glycolysis can perturb other cellular functions such as *de novo* fatty acid synthesis and ribose 5-phosphate for nucleotide synthesis[49].

The metabolic changes in Huh7 cells may be a contributor to the discrepancies between the cell line and hepatocytes *in vivo*[46]. Since the ECM can alter metabolisms in carcinoma cells including the energy pathways[50], we compared main metabolites of glycolysis and the Krebs cycle by LC-MS quantitation. As shown in **Fig. 2**, glucose-6-phosphate, fructose-6-phosphate, and glyceraldehyde-3-phosphate, three key metabolites in glycolysis, are significantly decreased in cells on the fibrous ECM, indicating reduced glycolysis. Malate, succinate, and α-ketoglutarate, three major metabolites in the Krebs cycle are also decreased. Perhaps due to the decreased glucose metabolism (i.e. glycolysis and the Krebs cycle), the glucose level in cells cultured on the ECM is higher. These data indicate that the ECM reduces energy metabolism in Huh7 cells, consistent with the notion that Huh7 cells cultured in 3D with the ECM take on the metabolic phenotype of hepatocytes in the liver.

The ECM changes amino acids bioavailability in Huh7 cells

Availability of amino acids, the building block of proteins, may also be affected by the ECM and the 3D culture. Indeed, compared to Huh7 cells cultured on a flat surface, those cultured on the ECM tend to have higher levels of amino acids, particularly tryptophan which is increased by >200% (**Fig. 3**). On the other hand, Huh7 cells cultured on the ECM have lower levels of spermine and methionine and similar levels of proline, creatine, and creatinine compared to those on a flat surface. Interestingly, indoleamine 2, 3-dioxygenase1, which degrades tryptophan and thus reduces tryptophan bioavailability, is overexpressed in human carcinoma hepatocyte cell lines including Huh7 compared to normal liver tissues[51, 52]. This may explain, at least in part, why tryptophan levels are lower in Huh7 cells grown on a flat surface. The concentrations of branched chain amino acids (BCAAs) including leucine, isoleucine, and valine are lower in carcinoma hepatocytes than in normal cells[53]. Other studies also suggest that increasing intracellular BCAAs can suppress the over-proliferation of carcinomic hepatocytes[54-56]. Our results show that the bioavailability of the three amino acids is increased in the cells culture on the fibrous ECM.

Methionine metabolism was found impaired in diseased hepatocytes including carcinoma, causing excessive methionine in both hepatocytes and in serum[57-59]. Our data in **Fig. 3** demonstrate that the fibrous ECM promotes methionine metabolism with reduced concentration of the molecule. Thus, at least for tryptophan, leucine/isoleucine, valine, and methionine, we conclude that the fibrous ECM modulates the bioavailability of these amino acids towards physiological relevance in Huh7 cells.

The ECM affects integrins expression

Protein kinase A (PKA), which is activated by cAMP, phosphorylates and inactivates key enzymes in glycolysis such as phosphofructokinase-2 and pyruvate kinase[60], thereby decreasing glycolysis. Also, Massimi et al. reported that increasing intracellular cAMP in a hepatic carcinoma cell line can repress its carcinomic characteristics[61]. Since glycolysis appears to be elevated in Huh7 cells on the flat stratum (**Fig. 2**), we first hypothesized that cAMP signaling may be suppressed in the cells cultured on the flat surface. Indeed, both cAMP level (**Fig. 4A**) and PKA activity, as measured by phosphorylation of the PKA substrate CREB (cAMP response element binding protein) (**Fig. 4B**), are reduced in Huh7 cells on the flat stratum.

The Huh7 cells from the same parental flask but cultured on the fibrous or flat ECMs have different morphologies. As shown in **Figs. 5A** and **5B**, the cells tend to grow into patches on both ECMs, but cells on the fibrous ECM appear to be larger with tighter junctions. The ECM fibers can also induce the formation of pseudopodia from the cells (**Fig. 5C**). Further analyses of the images reveal that the intercellular gaps between cells on the fibers is ~85% smaller than those on flat (**Fig. 5D**) while the cell size (area) ~15% larger (**Fig. 5E**).

It is not known how the fibrous ECM modulates intracellular cAMP levels and the cell morphology. We hypothesized that integrins may play a role because 1) integrins are the transmembrane receptor for ECMs which can transduce ECM signals; 2) overexpression of integrins can repress the cAMP levels in cytoplasm, reducing PKA activity[32-34], which was observed by us (**Fig. 6A**); 3) integrins overexpression increases actin polymerization, stress fiber formation and cellular contractility, which can reduce cell sizes and enlarge intercellular gaps[62, 63], correlating to our results in **Fig. 5**; and 4) integrins are mainly localized to the sites where cells bind the ECM (focal adhesion)[64], and the ECM microstructures affect focal adhesions[65].

Among the eight β subunits of integrin, β1 binds to the regular ECM components such as collagen and collagen-similar compounds[31]. As shown in **Fig. 6B**, Huh7 cells cultured on the ECM have reduced integrin β1 expression compared to those on the flat surface (**Fig. 6C**). These

results combined suggest that the fibrous ECM reduces the expression of integrins with increased downstream cAMP levels and actin depolymerization, which correlate the observed alterations of the basic metabolism in Huh7 cells.

Conclusion

Our work shows that the microfibrous ECM can reduce energy metabolites and increase the bioavailability of certain amino acids in Huh7 cell line. This effect of ECM fibers may be a result of downregulation of integrin expression which may increase the intracellular cAMP levels and control actin network formation. This is the first study reporting the effects of an ECM on the metabolites of hepatocytes cultured *in vitro*, and lays a groundwork for future hepatic modeling. Thus, this work enhances our understanding of the roles of ECM in controlling the integrin expression. The modular and translational cell culture technology that we developed should also facilitate future 3D cell culture research.

Acknowledgement

This work was supported by the startup funding of UMBC, and the Intramural Research Program of National Heart Lung and Blood Institute, National Institutes of Health. We thank the NHLBI Biochemistry Core and Dr. Duck-Yeon Lee's assistance for Mass Spectrometry, and the Keith Porter Imaging Center at UMBC.

Figures and Captions

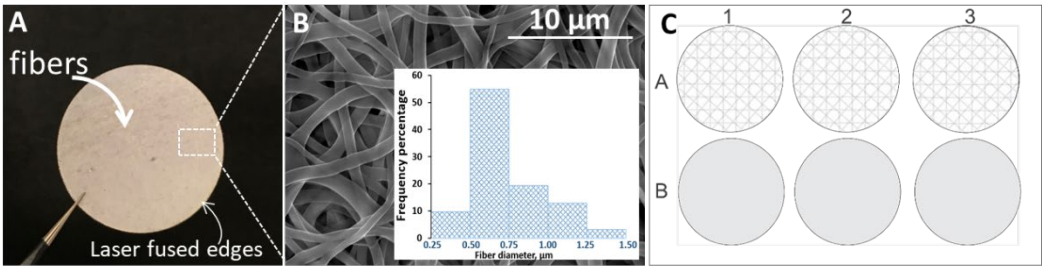

Figure 1.The research design. **(A)** Microfibers electrospun from silk fibroin were deposited on a polystyrene sheet, which was then laser cut to discs that can fit in a 6-well plate. **(B)** An SEM view of the electrospun fibers. Fiber diameter is 0.78±0.37µm (mean±stdev). The inset histogram shows the distribution of the fiber diameters. **(C)** Three discs with the microfiber ECM were placed in wells A1-3 while wells B1-3 contained flat-surface discs. Having controls in the same plate with cells being cultured and studied under the same environment will reduce possible variances.

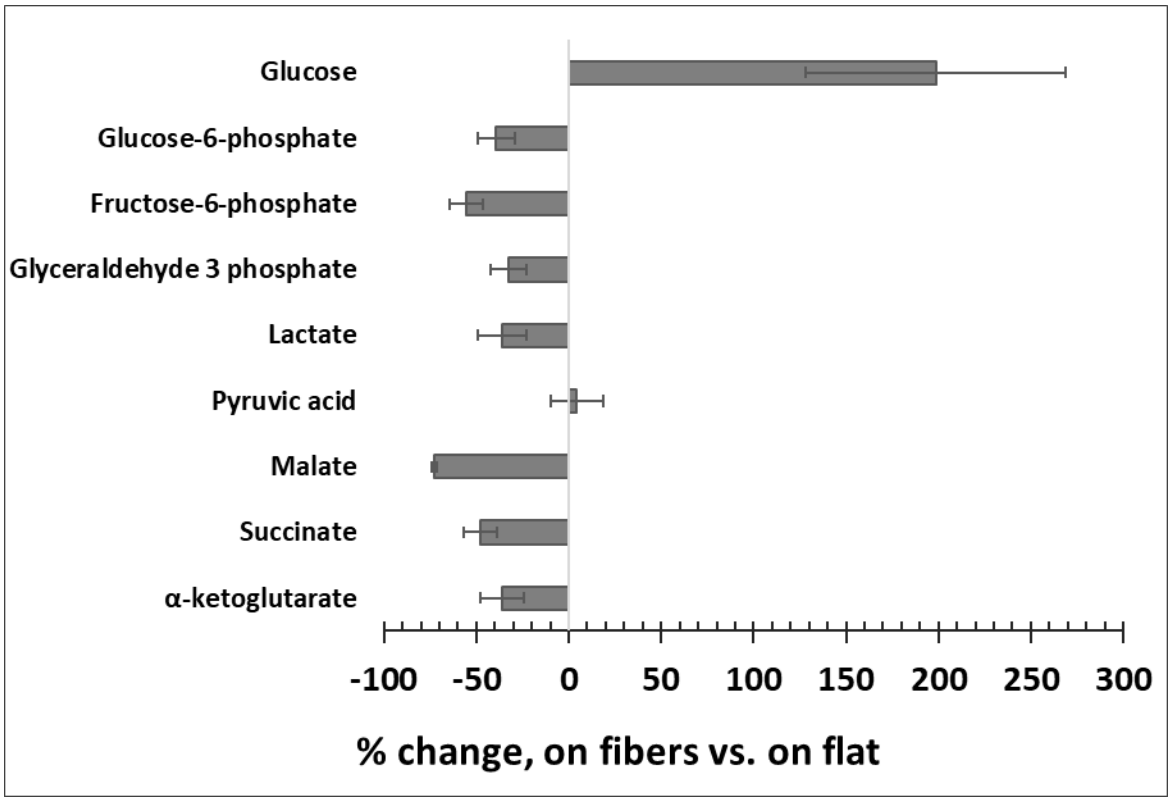

Figure 2. Energy metabolites in Huh7 cells cultured on the fibers vs. on a flat surface: 3 key metabolites in glycolysis and 3 key metabolites in the Kreb cycle were significantly decreased, indicating lower energy metabolism. As a main discrepancy compared to *in vivo*, Huh7 exibits extrelly elevated energy metabolism. Therefore, the suppressed energly metabolism on the fibrous ECM is more physiologically relevant. The glucose level is higher due to the reduced glycolytic metabolisms. N=15, error bar=S.E.M.

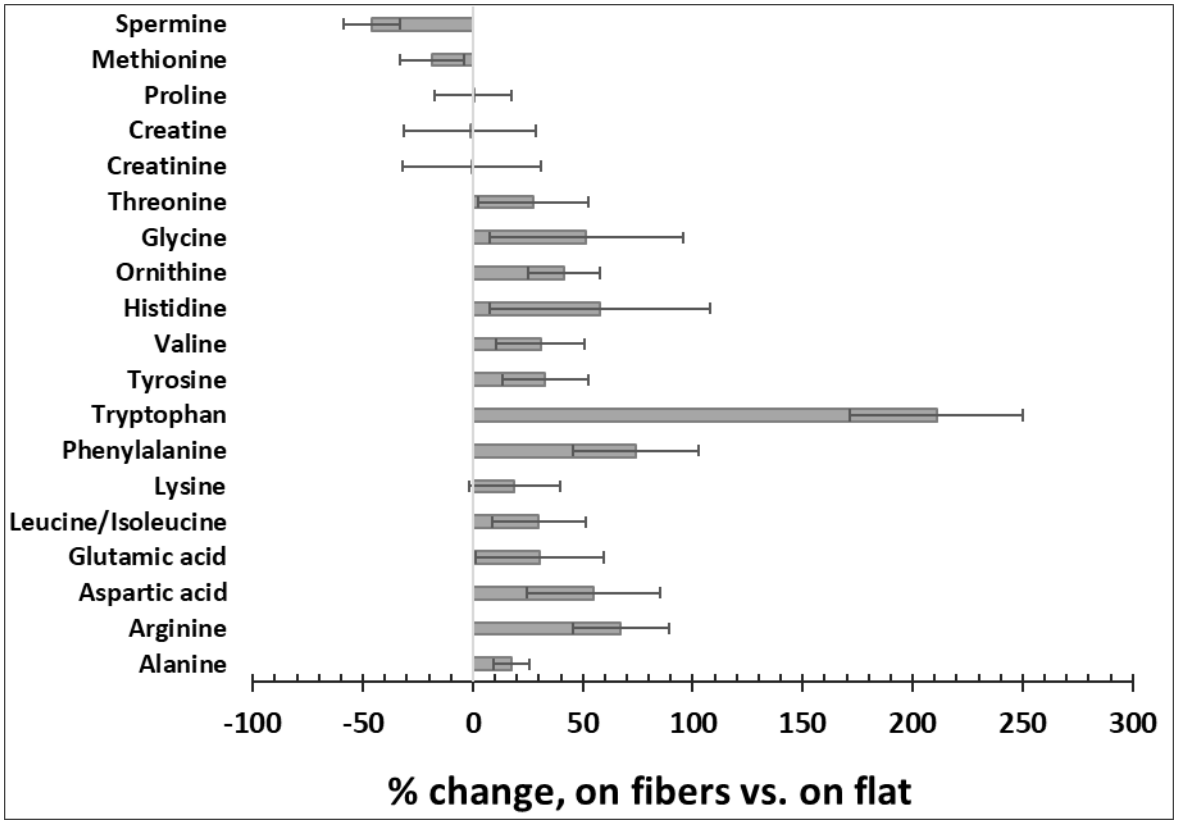

Figure 3. The bioavailability of most amino acids is higher in Huh7 cells on the fibers compared to on a flat surface, except for spermine, methionine, proline, creatine, and creatinine. Tryptophan shows a >200% increase. Studies prove that tryptophan is less abudent in Huh7 cells due to the over expression of Indoleamine 2, 3-Dioxygenase1. Our fibrous ECM makes intracellular tryptophan level more physiologically relevant. N=15, error bar=S.E.M.

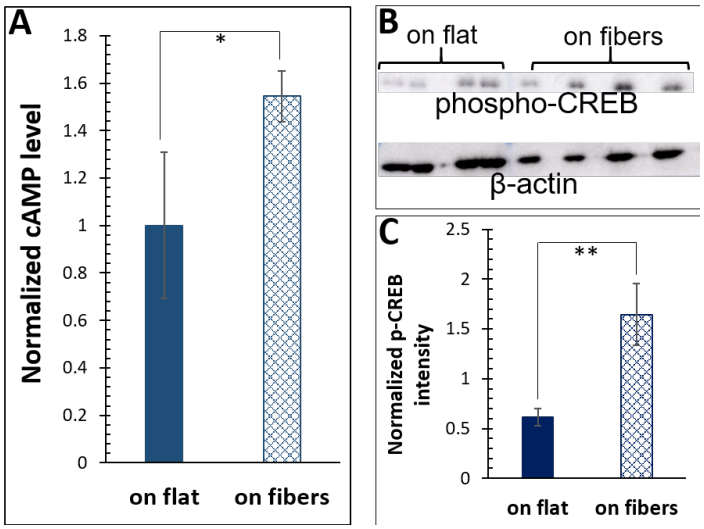

Figure 4. The effects of the ECM fibers on cAMP. **(A)** Huh7 cells cultured on the ECM fibers show significantly higher intracellular cAMP levels than those cultured on flat. N=6, error bar=S.E.M., *p<0.05. **(B)** The Western blot result of phosphorylated cAMP response element protein (CREP) in Huh7 cells cultured on flat vs. on the fibers. **(C)** Quantitation of the Western blot bands. Significantly more phosphorylated CREP was detected in cells on the fibers. N=8, **p<0.01.

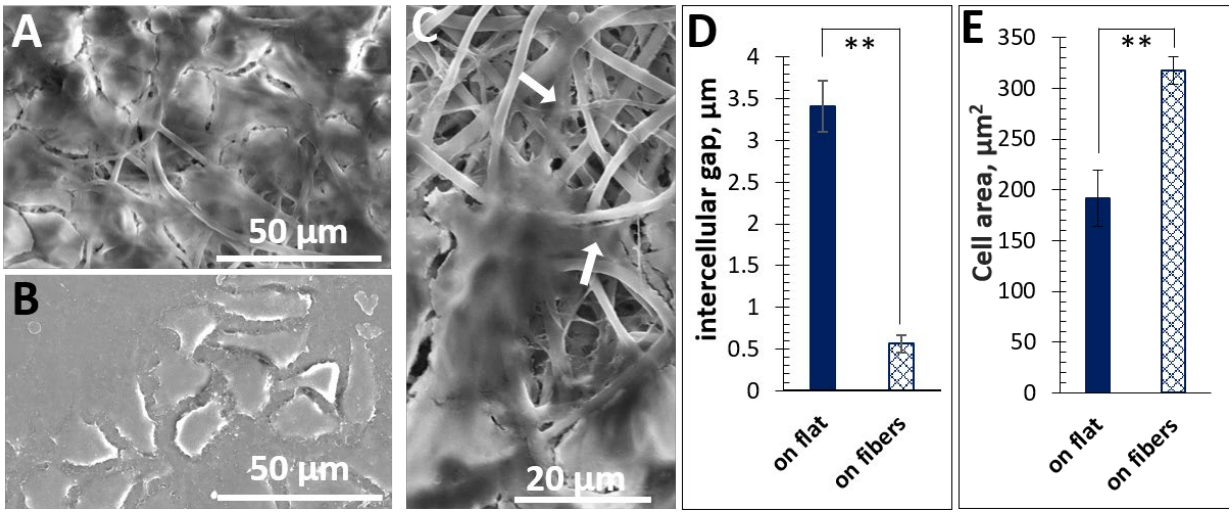

Figure 5. The effects of the ECM fibers on Huh7 cell morphology. **(A)** An SEM view of Huh7 cells on the fibrous ECM. **(B)** Huh7 cells cultured on a flat stratum. **(C)** Huh7 cells form pseudopodia structures to bind the fibers (arrows). **(D)** Cells on the 3D fibers are packed more tightly with smaller intercellular gaps. N=25, error bar=S.E.M., **P<0.01. **(E)** Cells cultured on the fibers and on flat have different sizes. Cells on the fibrous ECM are significantly larger. N=25, error bar=S.E.M., **p<0.01.

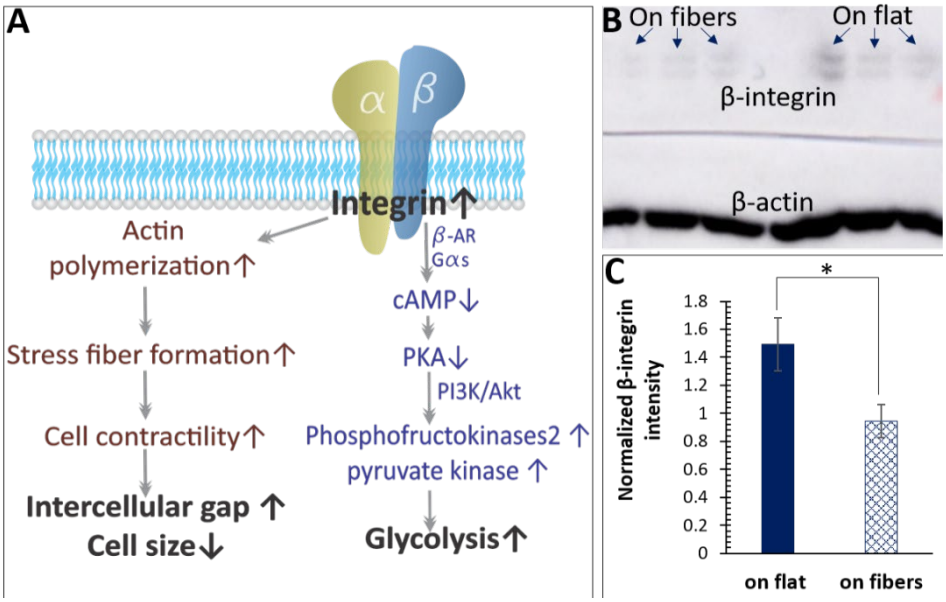

Figure 6. **(A)** Integrins on cell membrane can transduce ECM conditions to intracellular sygnaling. It has proven that overexpression of integrins can supress cAMP and its effector PKA, which in turn activates glycolytic enzymes and thus promotes glycolysis. Integrins overexpression can also lead to actin polymerization, causing cell contractility and thus enlarged intercellular gaps and shrank cell sizes. **(B)** A western-blot result of β-integrin1. Cells cultured on the flat stratum appears to express more integrins. **(C)** Quantitation of western-blot results show that the fibrous ECM significantly reduces the amount of integrins (N=7, *p<0.025).

References

[1] N. Fausto, J.S. Campbell, K.J. Riehle, Liver regeneration, *Hepatology,* **2006**, 43(2), S45-S53.
[2] N. Kaplowitz, Idiosyncratic drug hepatotoxicity, *Nature Reviews Drug Discovery,* **2005**, 4(6), 489-499.
[3] S.J. Haugabook, M. Ferrer, E.A. Ottinger, In vitro and in vivo translational models for rare liver diseases, *Biochimica Et Biophysica Acta-Molecular Basis of Disease,* **2019**, 1865(5), 1003-1018.
[4] M. Vinken, Liver-based in vitro models for toxicity testing, *Toxicology Letters,* **2018**, 295 S7-S7.
[5] S.M. Orbach, R.R. Less, A. Kothari, P. Rajagopalan, In Vitro Intestinal and Liver Models for Toxicity Testing, *Acs Biomaterials Science & Engineering,* **2017**, 3(9), 1898-1910.
[6] V.Y. Soldatow, E.L. LeCluyse, L.G. Griffith, I. Rusyn, In vitro models for liver toxicity testing, *Toxicology Research,* **2013**, 2(1), 23-39.
[7] B.G. Lake, J.A. Beamand, P.T. Wield, R.J. Price, Use of precision-cut liver slices to evaluate species differences in 2-acetylaminofluorene-induced unscheduled DNA synthesis, *Toxicology and Applied Pharmacology,* **1996**, 138(2), 231-241.
[8] V.M. Lauschke, R.Z. Shafagh, D.F.G. Hendriks, M. Ingelman-Sundberg, 3D Primary Hepatocyte Culture Systems for Analyses of Liver Diseases, Drug Metabolism, and Toxicity: Emerging Culture Paradigms and Applications, *Biotechnology Journal,* **2019**, 14(7).
[9] E. Ramboer, T. Vanhaecke, V. Rogiers, M. Vinken, Immortalized Human Hepatic Cell Lines for In Vitro Testing and Research Purposes, *Methods in Molecular Biology,* **2015**, 1250 53-76.
[10] F. Pati, J. Gantelius, H.A. Svahn, 3D Bioprinting of Tissue/Organ Models, *Angewandte Chemie-International Edition,* **2016**, 55(15), 4650-4665.
[11] A. Poloznikov, I. Gazaryan, M. Shkurnikov, S. Nikulin, O. Drapkina, A. Baranova, A. Tonevitsky, In Vitro and In Silico Liver Models: Current Trends, Challenges and Opportunities, *Altex-Alternatives to Animal Experimentation,* **2018**, 35(3), 397-412.
[12] K.F. Lei, C.H. Chang, M.J. Chen, Paper/PMMA Hybrid 3D Cell Culture Microfluidic Platform for the Study of Cellular Crosstalk, *Acs Applied Materials & Interfaces,* **2017**, 9(15), 13092-13101.
[13] Z.W. Chen, R.G. Zhao, Engineered Tissue Development in Biofabricated 3D Geometrical Confinement-A Review, *Acs Biomaterials Science & Engineering,* **2019**, 5(8), 3688-3702.
[14] D.B. Petropolis, D.M. Faust, M. Tolle, L. Riviere, T. Valentin, C. Neuveut, N. Hernandez-Cuevas, A. Dufour, J.C. Olivo-Marin, N. Guillen, Human Liver Infection in a Dish: Easy-To-Build 3D Liver Models for Studying Microbial Infection, *Plos One,* **2016**, 11(2).
[15] D.Y. No, K.H. Lee, J. Lee, S.H. Lee, 3D liver models on a microplatform: well-defined culture, engineering of liver tissue and liver-on-a-chip, *Lab on a Chip,* **2015**, 15(19), 3822-3837.
[16] L. Prodanov, R. Jindal, S.S. Bale, M. Hegde, W.J. McCarty, I. Golberg, A. Bhushan, M.L. Yarmush, O.B. Usta, Long-term maintenance of a microfluidic 3D human liver sinusoid, *Biotechnology & Bioengineering,* **2016**, 113(1), 241-6.
[17] K. Takayama, K. Kawabata, Y. Nagamoto, K. Kishimoto, K. Tashiro, F. Sakurai, M. Tachibana, K. Kanda, T. Hayakawa, M.K. Furue, H. Mizuguchi, 3D spheroid culture of hESC/hiPSC-derived hepatocyte-like cells for drug toxicity testing, *Biomaterials,* **2013**, 34(7), 1781-1789.
[18] N.S. Bhise, V. Manoharan, S. Massa, A. Tamayol, M. Ghaderi, M. Miscuglio, Q. Lang, Y.S. Zhang, S.R. Shin, G. Calzone, N. Annabi, T.D. Shupe, C.E. Bishop, A. Atala, M.R. Dokmeci, A. Khademhosseini, A liver-on-a-chip platform with bioprinted hepatic spheroids, *Biofabrication,* **2016**, 8(1).
[19] J.L. Guo, Y.S. Kim, A.G. Mikos, Biomacromolecules for Tissue Engineering: Emerging Biomimetic Strategies, *Biomacromolecules,* **2019**, 20(8), 2904-2912.
[20] E. Prince, M. Alizadehgiashi, M. Campbell, N. Khuu, A. Albulescu, K. De France, D. Ratkov, Y.F. Li, T. Hoare, E. Kumacheva, Patterning of Structurally Anisotropic Composite Hydrogel Sheets, *Biomacromolecules,* **2018**, 19(4), 1276-1284.

[21] L.L. Ouyang, C.B. Highley, C.B. Rodell, W. Sun, J.A. Burdick, 3D Printing of Shear-Thinning Hyaluronic Acid Hydrogels with Secondary Cross-Linking, *Acs Biomaterials Science & Engineering,* **2016**, 2(10), 1743-1751.
[22] N.R. Patel, A.K. Whitehead, J.J. Newman, M.E. Caldorera-Moore, Poly(ethylene glycol) Hydrogels with Tailorable Surface and Mechanical Properties for Tissue Engineering Applications, *Acs Biomaterials Science & Engineering,* **2017**, 3(8), 1494-1498.
[23] J.J. Xue, T. Wu, Y.Q. Dai, Y.N. Xia, Electrospinning and Electrospun Nanofibers: Methods, Materials, and Applications, *Chemical Reviews,* **2019**, 119(8), 5298-5415.
[24] M. Gholipourmalekabadi, S. Khosravimelal, Z. Nokhbedehghan, M. Sameni, V. Jajarmi, A.M. Urbanska, H. Mirzaei, M. Salimi, N.P.S. Chauhan, M. Mobaraki, R.L. Reis, A. Samadikuchaksaraei, S.C. Kundu, Modulation of Hypertrophic Scar Formation Using Amniotic Membrane/Electrospun Silk Fibroin Bilayer Membrane in a Rabbit Ear Model, *Acs Biomaterials Science & Engineering,* **2019**, 5(3), 1487-1496.
[25] J.H. Brown, P. Das, M.D. DiVito, D. Ivancic, L.P. Tan, J.A. Wertheim, Nanofibrous PLGA electrospun scaffolds modified with type I collagen influence hepatocyte function and support viability in vitro, *Acta Biomaterialia,* **2018**, 73 217-227.
[26] E.W.C. Chan, D. Bennet, P. Baek, D. Barker, S. Kim, J. Travas-Sejdic, Electrospun Polythiophene Phenylenes for Tissue Engineering, *Biomacromolecules,* **2018**, 19(5), 1456-1468.
[27] Y. Kang, C.L. Wang, Y.B. Qiao, J.W. Gu, H. Zhang, T. Peijs, J. Kong, G.C. Zhang, X.T. Shi, Tissue-Engineered Trachea Consisting of Electrospun Patterned scPLA/GO-g-IL Fibrous Membranes with Antibacterial Property and 3D-Printed Skeletons with Elasticity, *Biomacromolecules,* **2019**, 20(4), 1765-1776.
[28] S. Jin, F.H. Sun, Q. Zou, J.H. Huang, Y. Zuo, Y.B. Li, S.P. Wang, L. Cheng, Y. Man, F. Yang, J.D. Li, Fish Collagen and Hydroxyapatite Reinforced Poly(lactide-co-glycolide) Fibrous Membrane for Guided Bone Regeneration, *Biomacromolecules,* **2019**, 20(5), 2058-2067.
[29] N. Li, F.X. Xue, H. Zhang, H.J. Sanyour, A.P. Ricke, A. Uttecht, B. Fanta, J.L. Hu, Z.K. Hong, Fabrication and Characterization of Pectin Hydrogel Nanofiber Scaffolds for Differentiation of Mesenchymal Stem Cells into Vascular Cells, *Acs Biomaterials Science & Engineering,* **2019**, 5(12), 6511-6519.
[30] M. Mandon, S. Huet, E. Dubreil, V. Fessard, L. Le Hegarat, Three-dimensional HepaRG spheroids as a liver model to study human genotoxicity in vitro with the single cell gel electrophoresis assay, *Scientific Reports,* **2019**, 9.
[31] M. Barczyk, S. Carracedo, D. Gullberg, Integrins, *Cell and Tissue Research,* **2010**, 339(1), 269-280.
[32] A.M. Freyer, C.K. Billington, R.B. Penn, I.P. Hall, Extracellular matrix modulates beta(2)-adrenergic receptor signaling in human airway smooth muscle cells, *American Journal of Respiratory Cell and Molecular Biology,* **2004**, 31(4), 440-445.
[33] S.L. Lipsius, A.M. Samarel, beta(1)-integrins modulate beta-adrenergic receptor signaling, *Journal of Molecular and Cellular Cardiology,* **2004**, 36(6), 795-798.
[34] Q. Cheng, R.S. Ross, K.B. Walsh, Overexpression of the integrin beta(1A) subunit and the beta(1A) cytoplasmic domain modifies the beta-adrenergic regulation of the cardiac L-type Ca2+ current, *Journal of Molecular and Cellular Cardiology,* **2004**, 36(6), 809-819.
[35] D.N. Rockwood, R.C. Preda, T. Yucel, X.Q. Wang, M.L. Lovett, D.L. Kaplan, Materials fabrication from Bombyx mori silk fibroin, *Nature Protocols,* **2011**, 6(10), 1612-1631.
[36] A.K. Gutierrez-Garcia, M. Choudhury, A. De Leon-Rodriguez, Diisononyl Phthalate Differentially Affects Sirtuin Expression in the HepG2 Cell Line, *Chemical Research in Toxicology,* **2019**, 32(9), 1863-1870.
[37] H. Tamam, J. Park, H.H. Gadalla, A.R. Masters, J.A. Abdel-Aleem, S.I. Abdelrahman, A.A. Abdelrahman, L.T. Lyle, Y. Yeo, Development of Liposomal Gemcitabine with High Drug Loading Capacity, *Molecular Pharmaceutics,* **2019**, 16(7), 2858-2871.

[38] A. Harupa, L. De Las Heras, G. Colmenarejo, S. Lyons-Abbott, A. Reers, I. Caballero Hernandez, C.W. Chung, D. Charter, P.J. Myler, R.M. Fernandez-Menendez, F. Calderon, S. Palomo, B. Rodriguez, M. Berlanga, E. Herreros-Aviles, B.L. Staker, E. Fernandez Alvaro, A. Kaushansky, Identification of Selective Inhibitors of Plasmodium N-Myristoyltransferase by High-Throughput Screening, *Journal of Medicinal Chemistry,* **2020**, 63(2), 591-600.
[39] R. Rezaee, M. Abdollahi, The importance of translatability in drug discovery, *Expert Opinion on Drug Discovery,* **2017**, 12(3), 237-239.
[40] T. Agarwal, B. Subramanian, T.K. Maiti, Liver Tissue Engineering: Challenges and Opportunities, *Acs Biomaterials Science & Engineering,* **2019**, 5(9), 4167-4182.
[41] S. Breslin, L. O'Driscoll, Three-dimensional cell culture: the missing link in drug discovery, *Drug Discovery Today,* **2013**, 18(5-6), 240-249.
[42] V.J. Evans, N.M. Hawkins, B.B. Westfall, W.R. Earle, Studies on Culture Lines Derived from Mouse Liver Parenchymatous Cells Grown in Long-Term Tissue Culture, *Cancer Research,* **1958**, 18(3), 261-&.
[43] E.D. Hay, Cell Biology of Extracellular Matrix, *2nd edition,* **1991**.
[44] F. Pampaloni, E.G. Reynaud, E.H.K. Stelzer, The third dimension bridges the gap between cell culture and live tissue, *Nature Reviews Molecular Cell Biology,* **2007**, 8(10), 839-845.
[45] H. Moghadas, M.S. Saidi, N. Kashaninejad, A. Kiyoumarsioskouei, N.T. Nguyen, Fabrication and characterization of low-cost, bead-free, durable and hydrophobic electrospun membrane for 3D cell culture, *Biomedical Microdevices,* **2017**, 19(4).
[46] C.W. Pan, X.D. Wang, K.Q. Shi, Y. Zheng, J. Li, Y.P. Chen, L.X. Jin, Z.Z. Pan, MiR-122 Reverses the Doxorubicin-Resistance in Hepatocellular Carcinoma Cells through Regulating the Tumor Metabolism, *Plos One,* **2016**, 11(5).
[47] S. Cassim, V.A. Raymond, L. Dehbidi-Assadzadeh, P. Lapierre, M. Bilodeau, Metabolic reprogramming enables hepatocarcinoma cells to efficiently adapt and survive to a nutrient-restricted microenvironment, *Cell Cycle,* **2018**, 17(7), 903-916.
[48] L. Rui, Energy Metabolism in the Liver, *Compr Physiol,* **2014**, 4(1), 177-197.
[49] M.M. Adeva-Andany, N. Perez-Felpete, C. Fernandez-Fernandez, C. Donapetry-Garcia, C. Pazos-Garcia, Liver glucose metabolism in humans, *Bioscience Reports,* **2016**, 36.
[50] C.L. Buchheit, R.R. Rayavarapu, Z.T. Schafer, The regulation of cancer cell death and metabolism by extracellular matrix attachment, *Seminars in Cell & Developmental Biology,* **2012**, 23(4), 402-411.
[51] K. Pan, H. Wang, M.S. Chen, H.K. Zhang, D.S. Weng, J. Zhou, W. Huang, J.J. Li, H.F. Song, J.C. Xia, Expression and prognosis role of indoleamine 2,3-dioxygenase in hepatocellular carcinoma, *Journal of Cancer Research and Clinical Oncology,* **2008**, 134(11), 1247-1253.
[52] Q.Y. Zhao, P.P. Wang, Z.L. Huang, L. Peng, C.S. Lin, Z.L. Gao, S.C. Su, Tumoral indoleamine 2, 3-dioxygenase 1 is regulated by monocytes and T lymphocytes collaboration in hepatocellular carcinoma, *Oncotarget,* **2016**, 7(12), 14781-14790.
[53] K. Tajiri, Y. Shimizu, Branched-chain amino acids in liver diseases, *World Journal of Gastroenterology,* **2013**, 19(43), 7620-7629.
[54] K. Sugiyama, L. Yu, N. Nagasue, Direct effect of branched-chain amino acids on the growth and metabolism of cultured human hepatocellular carcinoma cells, *Nutr Cancer,* **1998**, 31(1), 62-8.
[55] M. Shimizu, S. Ninomiya, H. Moriwaki, Possible role of visfatin in hepatoma progression and the effects of branched-chain amino acids on visfatin-induced proliferation in human hepatoma cells, *Cancer Research,* **2012**, 72.
[56] S. Ninomiya, M. Shimizu, K. Imai, K. Takai, M. Shiraki, T. Hara, H. Tsurumi, S. Ishizaki, H. Moriwaki, Possible Role of Visfatin in Hepatoma Progression and the Effects of Branched-Chain Amino Acids on Visfatin-Induced Proliferation in Human Hepatoma Cells, *Cancer Prevention Research,* **2011**, 4(12), 2092-2100.

[57] E. Wainfan, M. Dizik, M. Stender, J.K. Christman, Rapid Appearance of Hypomethylated DNA in Livers of Rats Fed Cancer-Promoting, Methyl-Deficient Diets, *Cancer Research,* **1989**, 49(15), 4094-4097.
[58] L.W. Kinsell, H.A. Harper, H.C. Barton, G.D. Michaels, H.A. Weiss, Rate of Disappearance from Plasma of Intravenously Administered Methionine in Patients with Liver Damage, *Science,* **1947**, 106(2763), 589-590.
[59] J.H. Horowitz, E.B. Rypins, J.M. Henderson, S.B. Heymsfield, S.D. Moffitt, R.P. Bain, R.K. Chawla, J.C. Bleier, D. Rudman, Evidence for Impairment of Transsulfuration Pathway in Cirrhosis, *Gastroenterology,* **1981**, 81(4), 668-675.
[60] B. Wahlang, C. McClain, S. Barve, L. Gobejishvili, Role of cAMP and phosphodiesterase signaling in liver health and disease (Vol 49, pg 105, 2018), *Cellular Signalling,* **2019**, 53 414-414.
[61] M. Massimi, S. Cardarelli, F. Galli, M.F. Giardi, F. Ragusa, N. Panera, B. Cinque, M.G. Cifone, S. Biagioni, M. Giorgi, Increase of Intracellular Cyclic AMP by PDE4 Inhibitors Affects HepG2 Cell Cycle Progression and Survival, *Journal of Cellular Biochemistry,* **2017**, 118(6), 1401-1411.
[62] G.E. Davis, D.R. Senger, Endothelial extracellular matrix - Biosynthesis, remodeling, and functions during vascular morphogenesis and neovessel stabilization, *Circulation Research,* **2005**, 97(11), 1093-1107.
[63] K.A. DeMali, K. Wennerberg, K. Burridge, Integrin signaling to the actin cytoskeleton, *Current Opinion in Cell Biology,* **2003**, 15(5), 572-582.
[64] P. Uttayarat, G.K. Toworfe, F. Dietrich, P.I. Lelkes, R.J. Composto, Topographic guidance of endothelial cells on silicone surfaces with micro- to nanogrooves: Orientation of actin filaments and focal adhesions, *Journal of Biomedical Materials Research Part A,* **2005**, 75a(3), 668-680.
[65] H.N. Kim, J. Kim, Effect of Topographical Feature Size on the Trend of Cell Behaviors, *Ieee Transactions on Nanotechnology,* **2018**, 17(3), 377-380.